THERMAL EDGE-EFFECTS MODEL FOR AUTOMATED TAPE PLACEMENT OF THERMOPLASTIC COMPOSITES

Robert C. Costen
NASA Langley Research Center
Hampton, VA

ABSTRACT

Two-dimensional thermal models for automated tape placement (ATP) of thermoplastic composites neglect the diffusive heat transport that occurs between the newly placed tape and the cool substrate beside it. Such lateral transport can cool the tape edges prematurely and weaken the bond. The three-dimensional, steady state, thermal transport equation is solved by the Green's function method for a tape of finite width being placed on an infinitely wide substrate. The isotherm for the glass transition temperature on the weld interface is used to determine the distance inward from the tape edge that is prematurely cooled, called the cooling incursion Δa. For the Langley ATP robot, $\Delta a = 0.4$ mm for a unidirectional lay-up of PEEK/carbon fiber composite, and $\Delta a = 1.2$ mm for an isotropic lay-up. A formula for Δa is developed and applied to a wide range of operating conditions. A surprise finding is that Δa need not decrease as the Peclet number Pe becomes very large, where Pe is the dimensionless ratio of inertial to diffusive heat transport. Conformable rollers that increase the consolidation length would also increase Δa, unless other changes are made, such as proportionally increasing the material speed. To compensate for premature edge cooling, the thermal input could be extended past the tape edges by the amount Δa. This method should help achieve uniform weld strength and crystallinity across the width of the tape.

KEY WORDS: Modeling, Automated Tape Placement, Thermal Analysis

----

1. INTRODUCTION

The strength and high-temperature properties of carbon-fiber thermoplastic composites make them ideal for many structural applications. However, fabrication with these composites can be labor-intensive and costly. Automated tape placement (ATP) is a process designed to reduce this cost. In ATP, thermoplastic composite tape is placed on the previous layer and welded by heat and pressure to build up a laminated structure, as shown in Fig. 1.

Mathematical models have been developed to control and optimize the ATP process. Most of these models (refs. 1-10) are two-dimensional, as shown, for example, in Fig. 2. They restrict the heat transport to the x-y plane, and neglect the heat transport in the z-direction. In refs. 5-10, this two-dimensional approximation is justified partly by stating that the Peclet number $\mathrm{Pe} >> 1$, where Pe is the dimensionless ratio of inertial to diffusive heat transport. The present modeling study should determine if sufficiently large values of Pe do, indeed, justify the two-dimensional approximation.

If the applied heat q_0 is uniform across the tape width and zero outside, as shown in Fig. 1, a strong thermal gradient occurs in the substrate along the side edges of the tape. This thermal gradient can prematurely cool the tape edges and weaken the bond by causing heat to flow from the hot tape to the cool substrate beside it.

The main purpose of this study is to help achieve uniform weld strength and crystallinity across the width of the tape. For this purpose, the model will determine the prematurely cooled distance inward from the tape edge (the cooling incursion Δa) over a large range of processing parameters. This range includes the present operating condition of the ATP robot at Langley Research Center. The approach is to use the Green's function technique to obtain an analytic solution of the three-dimensional thermal transport problem shown in Fig. 1. Related studies at the *leading* edge of a new tape and at the *trailing* edge of a dropped tape are presented in refs. 8 and 9.

2. THREE-DIMENSIONAL MODEL

Figure 1 shows the steady state configuration where the laydown/consolidation head is fixed and the material moves with speed U beneath it. The Cartesian coordinate frame is fixed with the head, and its origin lies at the center of the nip line. The thermal input q_0 is directed at the nip line and is constant over the width of the tape $(-a \le z \le a)$ and zero elsewhere. Far away from the nip, the supporting tool and the head are both maintained at temperature T_∞, which is usually room temperature. The thermal input q_0 is constrained so that the temperature on the weld interface always decreases passively to the glass transition temperature T_g at the downstream end of the consolidation head x_h, where the pressure is released, as shown in Fig. 2. This constraint is enforced in the two-dimensional limit as $a \to \infty$

$$\lim_{a \to \infty} T(x_h, 0, z) = T_g \tag{1}$$

where z remains finite. In spite of this constraint, three-dimensional effects will cool the weld interface near the tape edge to T_g in a shorter distance than x_h.

The supporting tool and the head are taken to have the same thermal conductivity as the average thermal conductivity of the composite substrate. This assumption enables the configuration shown in Fig. 1 to be approximated by a line thermal source of length $2a$ that is fixed along the z-axis in an infinite moving conductor. The three-dimensional thermal transport equation then becomes

$$\rho C_p U \frac{\partial T}{\partial x} - K_{11}\frac{\partial^2 T}{\partial x^2} - K_{22}\frac{\partial^2 T}{\partial y^2} - K_{33}\frac{\partial^2 T}{\partial z^2} = q_0 \delta(x)\delta(y)\left[S(z+a) - S(z-a)\right] \tag{2}$$

where

ρ	density, kg m^{-3}
C_p	specific heat at constant pressure, J kg^{-1} K^{-1}
U	material speed in the positive x-direction, m s^{-1}
T	temperature, K
K_{11}, K_{22}, K_{33}	tensor conductivities along the x-, y-, and z-axes, W m^{-1} K^{-1}
q_0	thermal input power density at nip, W m^{-1}
$\delta(x), \delta(y)$	Dirac delta functions, m^{-1}
$S(z)$	Heaviside unit step function
a	Half width of tape, m

Dimensionless (primed) quantities are defined as follows:

$$T' \equiv \frac{T - T_\infty}{T_g - T_\infty} \tag{3a}$$

$$q_0' \equiv \frac{q_0}{2\pi (K_{11}K_{22})^{1/2}(T_g - T_\infty)} \tag{3b}$$

$$b \equiv \frac{\rho C_p U x_h}{2K_{11}} = \frac{\mathrm{Pe}}{2} \tag{3c}$$

$$x' \equiv \frac{x}{x_h}; \quad y' \equiv \left(\frac{K_{11}}{K_{22}}\right)^{1/2} \frac{y}{x_h}; \quad z' \equiv \left(\frac{K_{11}}{K_{33}}\right)^{1/2} \frac{z}{x_h} \tag{3d}$$

$$a' \equiv \left(\frac{K_{11}}{K_{33}}\right)^{1/2} \frac{a}{x_h} \tag{3e}$$

The partial derivatives become

$$\frac{\partial}{\partial x}=\frac{1}{x_h}\frac{\partial}{\partial x'} \tag{3f}$$

$$\frac{\partial}{\partial y}=\frac{1}{x_h}\left(\frac{K_{11}}{K_{22}}\right)^{1/2}\frac{\partial}{\partial y'} \tag{3g}$$

$$\frac{\partial}{\partial z}=\frac{1}{x_h}\left(\frac{K_{11}}{K_{33}}\right)^{1/2}\frac{\partial}{\partial z'} \tag{3h}$$

and (2) can be written

$$2b\frac{\partial T'}{\partial x'}-\frac{\partial^2 T'}{\partial x'^2}-\frac{\partial^2 T'}{\partial y'^2}-\frac{\partial^2 T'}{\partial z'^2}=q'(x',y',z') \tag{4a}$$

where

$$q'(x',y',z')=2\pi\, q_0'\delta(x')\delta(y')[S(z'+a')-S(z'-a')] \tag{4b}$$

subject to the boundary condition that $T'\to 0$ as $x', y',$ or $z'\to\infty$. In dimensionless variables, the constraint (1) becomes

$$\lim_{a'\to\infty} T'(1,0,z')=1 \tag{5}$$

where z' remains finite. In order to solve (4) in the infinite domain, an adjoint Green's function $H'(x',y',z'\,|\,x_0',y_0',z_0')$ is defined that satisfies the adjoint equation

$$-2b\frac{\partial H'}{\partial x'}-\frac{\partial^2 H'}{\partial x'^2}-\frac{\partial^2 H'}{\partial y'^2}-\frac{\partial^2 H'}{\partial z'^2}=\delta(x'-x_0')\delta(y'-y_0')\delta(z'-z_0') \tag{6}$$

where H' also vanishes at infinity. Multiplying (4a) by H' and (6) by T', subtracting, and integrating by parts over the infinite x',y',z'-domain gives

$$T'(x_0',y_0',z_0')=\int_{-\infty}^{\infty}dx'\int_{-\infty}^{\infty}dy'\int_{-\infty}^{\infty}dz'\,q'(x',y',z')H'(x',y',z'\,|\,x_0',y_0',z_0') \tag{7}$$

Equation (6) can be solved by the method of Fourier transforms to obtain the adjoint Green's function

$$H'\left(x',y',z'\,|\,x_0',y_0',z_0'\right)=\frac{\exp\left(-b\left\{\left[\left(x'-x_0'\right)^2+\left(y'-y_0'\right)^2+\left(z'-z_0'\right)^2\right]^{1/2}+\left(x'-x_0'\right)\right\}\right)}{4\pi\left[\left(x'-x_0'\right)^2+\left(y'-y_0'\right)^2+\left(z'-z_0'\right)^2\right]^{1/2}} \tag{8}$$

If the x',y',z'-variables are interchanged with the x_0',y_0',z_0'-variables, equations (7), (4b), and (8) become

$$T'\left(x',y',z'\right)=\int_{-\infty}^{\infty}dx_0'\int_{-\infty}^{\infty}dy_0'\int_{-\infty}^{\infty}dz_0'\,q'\left(x_0',y_0',z_0'\right)H'\left(x_0',y_0',z_0'\,|\,x',y',z'\right) \tag{9a}$$

where

$$q'\left(x_0',y_0',z_0'\right)=2\pi\,q_0'\,\delta(x_0')\delta(y_0')\left[S\left(z_0'+a'\right)-S\left(z_0'-a'\right)\right] \tag{9b}$$

$$H'\left(x_0',y_0',z_0'\,|\,x',y',z'\right)=\frac{\exp\left(-b\left\{\left[\left(x_0'-x'\right)^2+\left(y_0'-y'\right)^2+\left(z_0'-z'\right)^2\right]^{1/2}+\left(x_0'-x'\right)\right\}\right)}{4\pi\left[\left(x_0'-x'\right)^2+\left(y_0'-y'\right)^2+\left(z_0'-z'\right)^2\right]^{1/2}} \tag{9c}$$

Substituting (9b) and (9c) into (9a) and integrating gives

$$T'\left(x',y',z'\right)=\frac{q_0'}{2}\int_{-a'}^{a'}dz_0'\,\frac{\exp\left(-b\left\{\left[x'^2+y'^2+\left(z_0'-z'\right)^2\right]^{1/2}-x'\right\}\right)}{\left[x'^2+y'^2+\left(z_0'-z'\right)^2\right]^{1/2}} \tag{10}$$

As mentioned, the dimensionless thermal input q_0' is determined by the constraint (5). If (10) is substituted into (5) and the identification is made that

$$K_0(b)=\frac{1}{2}\int_{-\infty}^{\infty}du'\,\frac{\exp\left[-b\left(1+u'^2\right)^{1/2}\right]}{\left(1+u'^2\right)^{1/2}} \tag{11}$$

where u' is a dummy variable of integration and $K_0(b)$ is a hyperbolic Bessel function, then

$$q_0'=\frac{1}{\exp(b)K_0(b)} \tag{12}$$

The dimensionless temperature field (10) becomes finally

$$T'(x',y',z') = \frac{1}{2\exp(b)K_0(b)} \int_{-a'}^{a'} dz_0' \frac{\exp\left(-b\left\{\left[x'^2+y'^2+(z_0'-z')^2\right]^{1/2}-x'\right\}\right)}{\left[x'^2+y'^2+(z_0'-z')^2\right]^{1/2}} \tag{13}$$

Note that this solution depends on only two dimensionless parameters: b and the dimensionless half-width a'.

3. ISOTHERMS ON THE WELD INTERFACE

As shown in Figs. 1 and 2, the weld interface occurs on the plane $y'=0$. Equation (13) can be used to plot the isotherms of dimensionless temperature T' on this plane. (Computations are actually done on the plane $y'=0.001$ to avoid the infinite temperature along the nip line ($x'=0,\ y'=0, -a'\le z'\le a'$).)

The interface isotherms are plotted in Fig. 3 for $a'=1.5$ and three values of b. The value $b=10$ corresponds to the present operating condition of the Langley ATP robot. Cooling along the edge of the tape $(z'=a'=1.5)$ is clearly evident. In the absence of this cooling, the isotherm $T'=1$ would lie on $x'=1$ across the full width of the tape, in accordance with the constraint (5).

The $T'=1$ isotherm, which corresponds to the glass transition temperature, is used to quantify the dimensionless cooling incursion $\Delta a'$, as follows: The dimensionless distance from the tape edge $(z'=a'=1.5)$ to the point where the $T'=1$ isotherm reaches $x'=1$ defines $\Delta a'$. As shown in Figs. 3(b) and 3(c), $\Delta a'$ decreases as b increases. In fact, $\Delta a'$ is purely a function of b. The dependence of $\Delta a'$ on b, as determined numerically from (13), is plotted in Fig. 4.

The cooling incursion Δa (in m) is then determined from the inverse of (3e)

$$\Delta a = \left(\frac{K_{33}}{K_{11}}\right)^{1/2} x_h \Delta a' \tag{14}$$

Also plotted in Fig. 4 is an approximate formula for $\Delta a'(b)$, given by

$$\Delta a' \approx \frac{1.66}{b}\left[1-\tanh(.11b-10)\right] + \frac{1.415}{\sqrt{b}}\left[1+\tanh(.104b-.4)\right] \tag{15}$$

Substitution of this formula (15) and (3c) into (14) then gives

$$\Delta a \approx \frac{3.32(K_{11}K_{33})^{1/2}}{\rho C_p U}\left[1-\tanh(.11b-10)\right] + 2\left(\frac{K_{33}x_h}{\rho C_p U}\right)^{1/2}\left[1+\tanh(.104b-.4)\right] \tag{16}$$

where Δa (in m) is the cooling incursion inward from the tape edge. For $b > 10$, the second term on the right hand side is dominant, and (16) can be written

$$\Delta a \approx 4\left(\frac{K_{33}x_h}{\rho C_p U}\right)^{1/2} \qquad (b > 10) \qquad (17)$$

4. EXAMPLE

This example illustrates the application of (14)-(16) and Fig. 4. It starts from the present operating condition of the Langley ATP robot, where the consolidation length $x_h = 1.27\times10^{-3}$ m and the speed $U = 0.0425$ m s^{-1}. For PEEK/carbon fiber tape laid-up unidirectionally, the thermal conductivity components are given by $K_{11} = 6$ W m^{-1} K^{-1} and $K_{22} = K_{33} = 0.72$ W m^{-1} K^{-1}. The density and specific heat are given by $\rho = 1560$ kg m^{-3} and $C_p = 1425$ J kg^{-1} K^{-1}. Substituting these values in (3c) gives $b = 10$. Figure 4 or, alternatively, equation (15) then gives $\Delta a' = 1$. Substitution in (14) or (16) finally gives the cooling incursion inward from the edge of the tape as $\Delta a = 0.4$ mm. This point is plotted on the lower curve of Fig. 5.

As the performance of the Langley robot is upgraded in the future, both U and x_h will increase. The increase in x_h results from a desire to make the consolidation roller more conformable. Also, increasing x_h increases the effective bonding time, as show by sensitivity studies presented in ref. 10. Suppose that both U and x_h are doubled. Then $b = 40$ and a second point can be calculated and plotted on the lower curve of Fig. 5. This entire curve is obtained by proportionally increasing (or decreasing) U and x_h from the initial point $(b = 10)$.

If successive layers are angled to make the composite substrate isotropic, the average values of the conductivity components become $K_{11} = K_{33} = 3.36; K_{22} = .72$. Recalculation with these values (and recalling that b depends on K_{11}) gives the upper curve in Fig. 5, where the minimum cooling incursion $\Delta a = 1.2$ mm.

5. DISCUSSION

A comparison of Figs. 4 and 5 shows that, although $\Delta a'$ is a decreasing function of b, Δa levels off for $b > 10$. Equation (17), which is valid for $b > 10$, provides the following explanation: If U and x_h are increased proportionally, as done in the example shown in Fig. 5, then Δa remains constant when $b > 10$.

The range $(b > 10)$ is of great interest in ATP. Increases in the speed U benefit the productivity of a unit, and increases in x_h are a natural consequence of the trend toward using conformable rollers. As shown by (17), however, increasing x_h has the undesirable effect of increasing the cooling incursion Δa. A rearrangement of the plies that increases the average value of K_{33} also increases Δa, as does any decrease in the density ρ or the specific heat C_p. To counteract these adverse effects on Δa, U could be simultaneously increased, as exemplified in Fig. 5.

Equation (17) shows clearly that for $b > 10$ the cooling incursion Δa need not decrease as the Peclet number $\mathrm{Pe} = 2b = \rho C_p U x_h / K_{11}$ increases. If the increase in Pe is due solely to a decrease in K_{11}, Δa will not be changed. If the increase in Pe is due solely to an increase in x_h, Δa will actually increase. Therefore, large values of Pe do not necessarily justify the use of a two-dimensional approximation in ATP thermal transport models.

A simple fix for the tape-edge cooling problem is to extend the thermal input past the tape edges by the amount Δa, as given by (14), (16) or (17). This approach should help achieve uniform strength and crystallinity across the width of the tape. Of course, extending the thermal input past the tape edges would cause some substrate reheating as the tape is repetitively placed side-by-side. Such reheating must be minimized to reduce thermal degradation. Formulas (14), (16), and (17) should help provide these minimum values.

6. CONCLUSIONS

The idealized three-dimensional thermal transport problem for the ATP configuration shown in Fig. 1 was found to have a relatively simple analytic solution (13) for the dimensionless temperature $T'(x', y', z')$. This solution depends on only two parameters, $b = \mathrm{Pe}/2$, where Pe is the Peclet number, and the dimensionless tape half-width a'. Plots of the dimensionless isotherms on the weld interface reveal premature cooling along the side edge of the tape. This cooling results from the large thermal gradient between the newly placed tape and the cool substrate beside it.

The prematurely cooled dimensionless distance inward from the tape edge $\Delta a'$ was determined from the $T' = 1$ isotherm, which corresponds to the glass transition temperature T_g. The inward sweep of this isotherm at the downstream end of the consolidation head, where $x_h' = 1$, defines $\Delta a'$. As determined numerically, $\Delta a'$ was found to be a monotonically decreasing function of b alone.

An approximate formula for $\Delta a'(b)$ was also found (15). This formula was then inverted to give the cooling incursion Δa (in m). For the important range $b > 10$, the formula for Δa reduces to a simple form (17). This simple form shows, surprisingly, that large values of the Peclet number $\mathrm{Pe} = 2b$ do not necessarily justify the two-dimensional thermal approximation that is often used in ATP models.

For the Langley ATP robot, presently operating at $b = 10$ with PEEK/carbon fiber composite, the cooling incursion is in the range $(0.4\,\mathrm{mm} \le \Delta a \le 1.2\,\mathrm{mm})$. The lower value corresponds to a unidirectional lay-up, and the higher value to an isotropic lay-up. An upgrade in roller conformability that increases the consolidation length x_h would increase Δa unless a compensating change is made, such as proportionally increasing the material speed.

A simple fix for the tape-edge cooling problem is to extend the thermal input past the tape edges by the amount Δa, as given by formulas (14, (16), or (17). This approach should help achieve uniform weld strength and crystallinity across the width of the tape.

7. REFERENCES

1. F. O. Sonmez and H. T. Hahn, *J. Thermoplastic Composite Materials, 10*, 198-240 (1997).
2. R. Pitchumani, S. Ranganathan, R. C. Don, J. W. Gillespie, Jr., and M.A. Lamontia, *Int. J. Heat Mass Transfer, 39*, 1883-1897 (1996).
3. H. Sarrazin and G. S. Springer, *J. Composite Materials, 29,* 1908-1943 (1995).
4. R. G. Irwin, Jr. and S. I. Güçeri, *AMD-Vol. 194, Mechanics in Materials Processing and Manufacturing*, ASME, 319-333 (1994).
5. E. P. Beyeler and S. I. Güçeri, *Trans. ASME, 110*, 424-430 (1988).
6. M. N. G. Nejhad, R. D. Cope, and S. I. Güçeri, *J. Thermoplastic Composite Materials, 4*, 20-45 (1991).
7. S. M. Grove, *Composites, 19*, 367-375 (1988).
8. R. C. Costen and J. M. Marchello, *SAMPE International Symposium, 44*, 1820-1830 (1999).
9. R. C. Costen and J. M. Marchello, *SAMPE International Symposium, 43*, 2005-2019 (1998).
10. R. C. Costen and J. M. Marchello, *SAMPE International Symposium, 42*, 33-47 (1997).

BIOGRAPHY

Robert C. Costen is an applied mathematician at NASA-Langley who works in the Advanced Materials and Processing Branch. He has authored and co-authored numerous modeling papers in materials processing, aerodynamics, atmospheric science, lasers, and radiation protection**.**

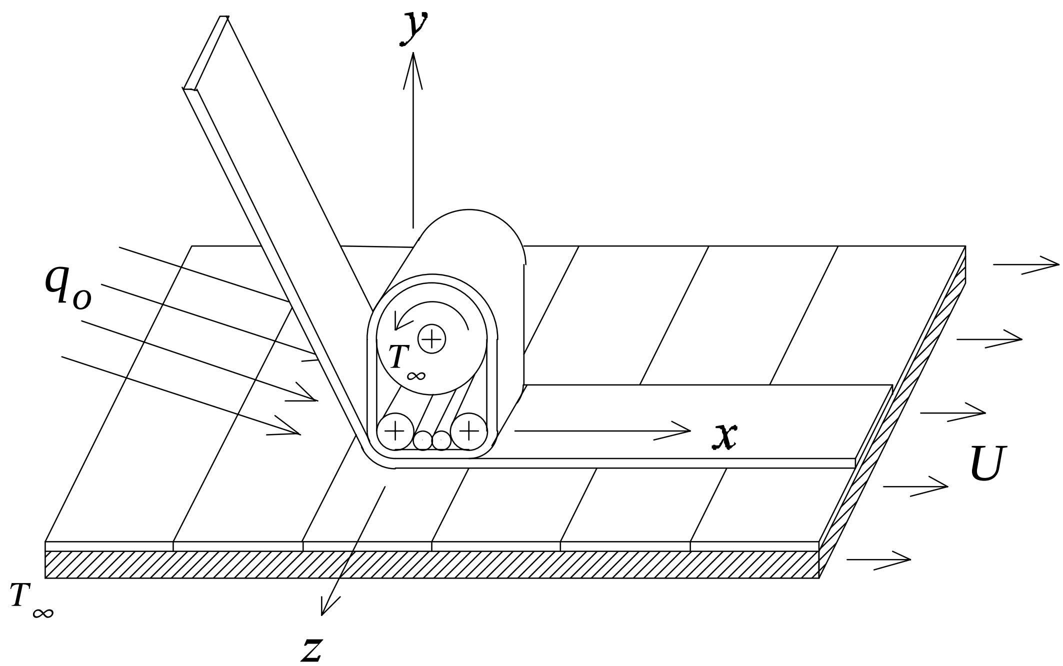

Figure 1. Three-dimensional sketch of the automated tape placement (ATP) process. Heat q_0 is directed at the nip (the line defined by the z-axis) and distributed uniformly over the width of the tape $(-a \le z \le a)$. Pressure is applied over the distance $(0 \le x \le x_h)$.

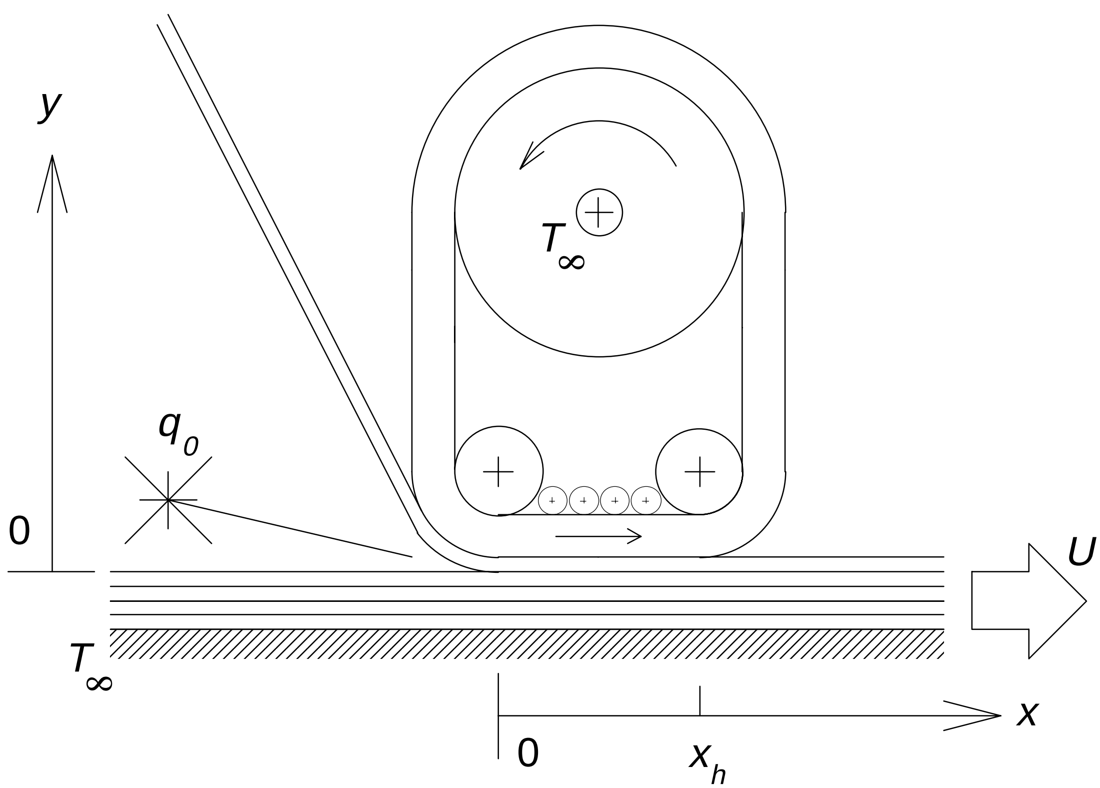

Figure 2. Two-dimensional approximation to the three-dimensional model shown in Fig. 1.

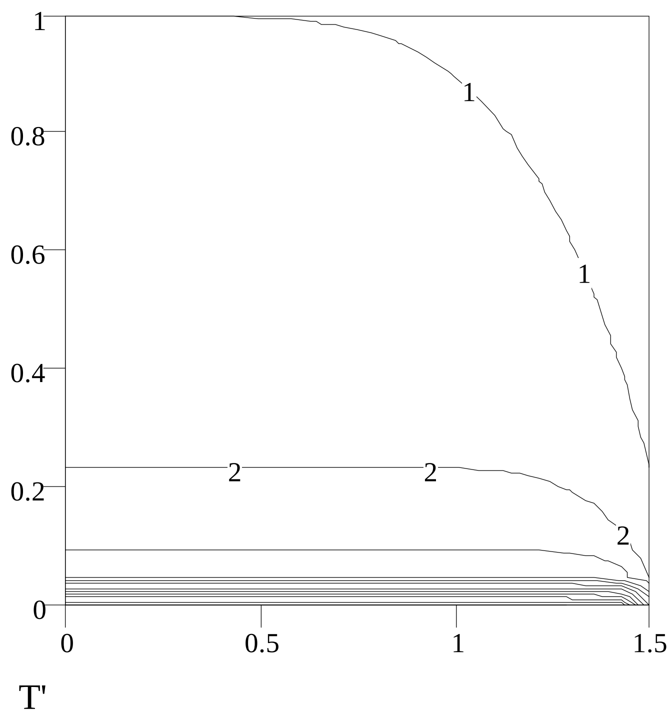

(a) $b = 10$

Figure 3. Isotherms of dimensionless temperature T' on the weld interface ($x'-z'$ plane) for dimensionless half-width $a' = 1.5$ and various b. The x'-axis (vertical axis) lies along the centerline of the tape. The edge of the tape is at $z' = a' = 1.5$. Consolidation ends at $x' = 1$.

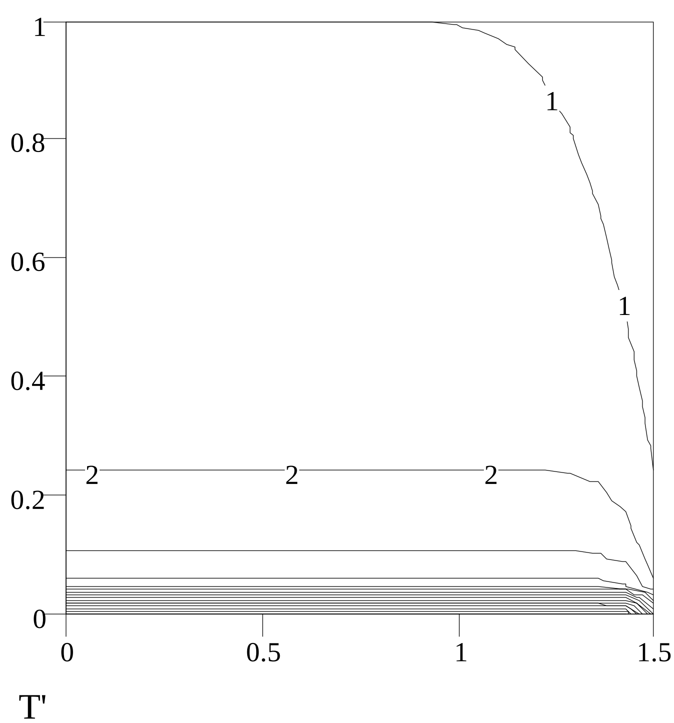

(b) $b = 31.6$

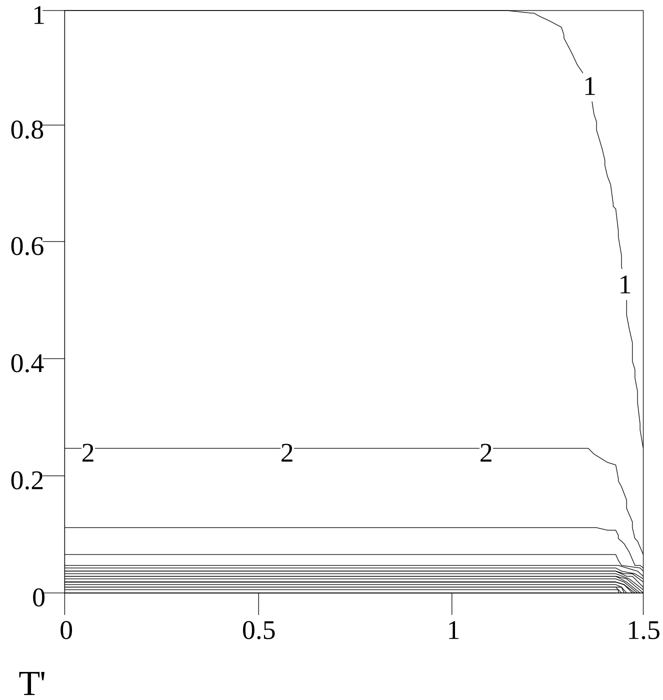

(c) $b = 100$

Figure 3. Concluded.

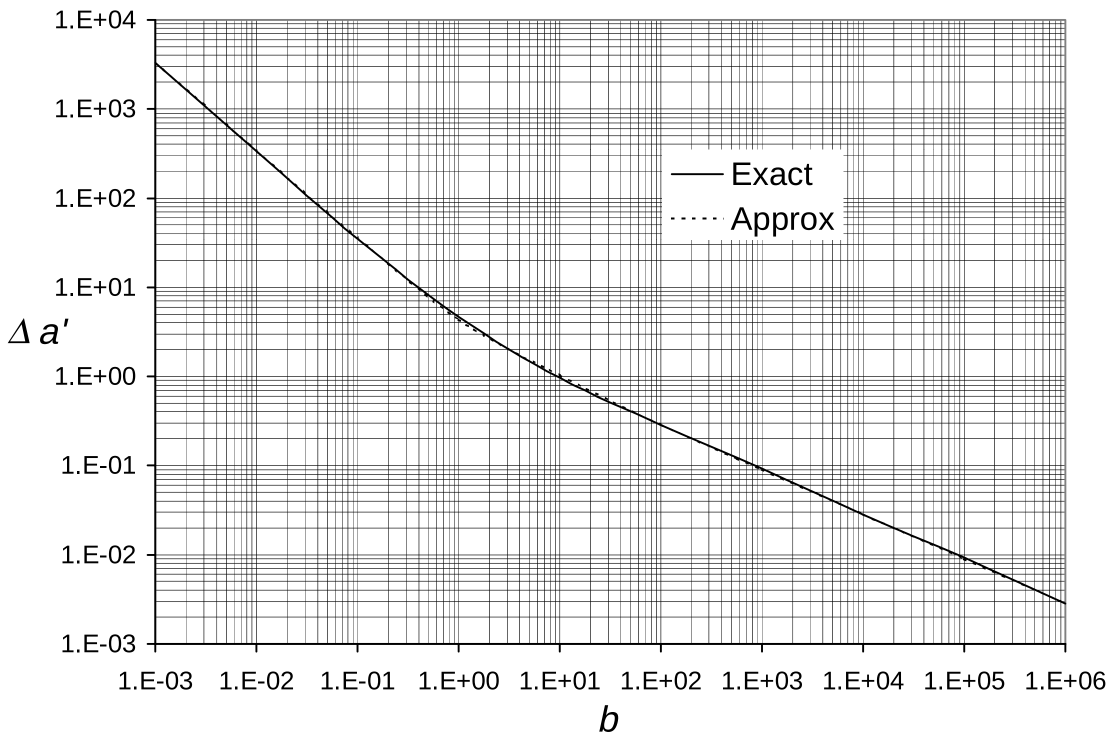

Figure 4. Dimensionless distance inward from tape edge affected by premature cooling $\Delta a'$ vs. b. Approximate curve is from equation (15).

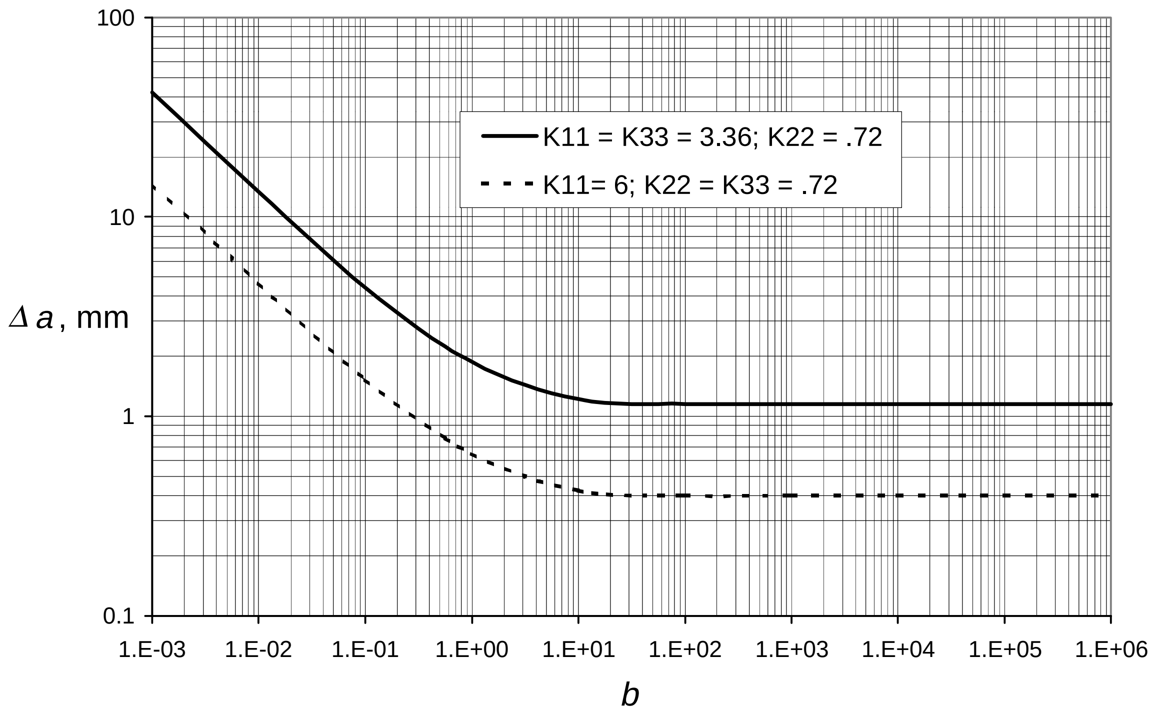

Figure 5. Distance inward from tape edge affected by premature cooling (the cooling incursion) Δa vs. b for the example presented in section 4.